FINAL TECHNICAL REPORT

USGS AWARD G16AP00117

Earthquake rupture propagation into creeping areas of the San Andreas Fault

Principal Investigator: Nadia Lapusta, California Institute of Technology
1200 E. California Blvd., Pasadena, CA 91125
(626) 395-2277, Fax: (626) 568-2719, lapusta@caltech.edu

Abstract

Faults experience both slow slip and fast, seismic-wave producing, rupture events perceived as earthquakes. These behaviors are often assumed to be separated in space and to occur on two different types of fault segments: one with stable, rate-strengthening, friction and the other with rate-weakening friction that leads to stick-slip. Our group has developed models in which stable, rate-strengthening behavior at low slip rates is combined with coseismic weakening, allowing unstable slip to occur in segments which can also creep between events. The implication that earthquake rupture may break through large portions of creeping segments - currently perceived as barriers - requires re-evaluation of seismic hazard in many areas, including California.

In this project, we have explored the seismological and geodetic observables in fault models that allow for earthquake penetration into deeper, stably creeping fault extensions. Our modeling suggest that the transition between the locked and fully creeping regions in such models can occur over a broad depth range. The effective locking depth, D_{elock}, associated with concentrated loading and promotion of microseismicity, is located near the top of this transition zone; the geodetic locking depth, D_{glock}, inverted from surface geodetic observations, corresponds to the depth of fault creeping with approximately half of the long-term rate. Following large earthquakes, D_{elock} either stays in place or becomes shallower due to creep penetrating into the shallower locked areas, whereas D_{glock} deepens as the slip deficit region expands, compensating for the afterslip. As the result, the two locking depths diverge in the late interseismic period, consistent with available seismic and geodetic observations from several major fault segments in Southern California. We find that D_{glock} provides a bound on the depth limit of large earthquakes in our models.

We have also examined the effect of dynamic weakening on the source properties and interaction of the SF and LA repeaters, the targets of the SAFOD observatory. One of the goals of our modeling is to reproduce the relatively high inferred stress drops of these repeaters (~30 MPa), which correspond to patch sizes consistent with the high degree of interaction of the SF and LA repeaters without overlapping of their sources. To that end, we augment the standard rate-and-state model for the repeaters in two ways: by adding enhanced coseismic weakening in the form of thermal pressurization of pore fluids to the VW patch (M1) and by imposing locally elevated normal stress on the VW patch (M2). We find that both models can reasonably closely reproduce the source properties of the SF and LA repeaters, including the inferred relatively high stress drops, moment magnitude, recurrence interval, and triggering time of the interaction. The models also place constraints on the properties of the surrounding velocity-strengthening region, an important contribution towards our ongoing work of using models to determine whether the creeping segment can be dynamically ruptured. We have also started to explore the role of heterogeneity of friction properties as well as to develop a methodology for comparing our sources to seismological observations more directly.

The studies have put constraints on the properties of parts of the SAF; advanced our understanding of the types of frictional behavior relevant to fault slip, earthquake interaction, and earthquake nucleation

and triggering; and will eventually contribute to the evaluation of seismic hazard in California. The resulting better understanding of fault physics and seismic hazard will contribute to reduction of losses from earthquakes in the US. The research is well-aligned with the USGS Priority Topics in Research on Earthquake Physics.

Publications and presentations of research supported by this project:

Jiang, J., and N. Lapusta, Connecting depth limits of interseismic locking, microseismicity, and large earthquakes in models of long-term fault slip, revision submitted to *J. Geophys. Res.*, 2017.

Lui, S.K.Y., and N. Lapusta, Modeling high stress drops, interaction, and irregularity of repeating SF and LA earthquake sequences on the San Andreas fault, to be submitted to *J. Geophys. Res.*, 2017.

Higgins, N., and N. Lapusta, Asperity-Type Foreshock Sources Driven by Nucleation-Induced Creep within a Rate-and-State Fault Model, *AGU Fall Meeting*, San Francisco, CA, Dec. 2016. (Oral presentation)

Jiang, J., and N. Lapusta, Variability of earthquake slip and arresting depths in fault models (oral presentation), *The 24th International Congress of Theoretical and Applied Mechanics*, Montréal, Québec, Canada, Aug. 2016. (Oral presentation)

Jiang, J., Fialko, Y. and N. Lapusta, Can interseismic geodetic observations and microseismicity shed light on large earthquake behavior? Insights from models of long-term fault slip, SSA Annual Meeting, Denver, CO, Apr. 2017.

Lin, Y.-Y., and N. Lapusta, Exploring variations of earthquake moment on patches with heterogeneous strength, *AGU Fall meeting*, San Francisco, CA, Dec. 2016. (Oral presentation)

Lui, S.K.Y., and N. Lapusta, Physics-based elastodynamic modeling of interacting frictional shear cracks, *The 24th International Congress of Theoretical and Applied Mechanics*, Montréal, Québec, Canada, Aug. 2016. (Oral presentation)

Perry, S. and N. Lapusta. Reproducing magnitude-invariant stress drops in fault models with thermal pressurization (oral presentation), *The 24th International Congress of Theoretical and Applied Mechanics*, Montréal, Québec, Canada, Aug. 2016. (Oral presentation)

1. Models of fault slip with rate-and-state friction and dynamic weakening

Our studies supported by USGS have resulted in fault models capable of reproducing a number of observations on the San Andreas fault, such as scaling of small repeating earthquakes, their response to postseismic slip, relatively large stress drops and interaction of the LA and SF repeaters, quasi-periodic recurrence of the Mw 6 events and the associated post- and interseismic slip, and different behavior of microseismicity on different fault segments and the associated possibility of deeper penetration of large earthquakes (Chen and Lapusta, 2009; Chen et al., 2010; Barbot et al., 2012; Jiang and Lapusta, 2016, 2017; Lui and Lapusta, 2016, 2017). The models and their extensions have been used to explore the potential for and consequences of deeper penetration of earthquake rupture into creeping fault extensions and the potential for dynamic rupture to propagate through creeping segments (Noda and Lapusta, 2013; Jiang and Lapusta, 2016, 2017; ongoing work).

Our models include two aspects of earthquake source physics that have been gaining acceptance and validation through laboratory experiments and comparison of earthquake models with observations.

The first one is the rate-and-state nature of fault friction at low, aseismic slip rates, conclusively documented in laboratory experiments and used to reproduce, both qualitatively and quantitatively, a number of earthquake-source observations (Dieterich, 2007; Scholz, 1998). Our previous studies supported by USGS have shown that the standard logarithmic rate and state formulations (Dieterich,

1979, 1981; Ruina, 1983; Blanpied et al., 1991, 1995; Beeler et al., 1994; Marone, 1998) allow us to match a number of basic observations regarding repeating earthquakes in the creeping section and quasi-period Mw 6 events (Chen and Lapusta, 2009; Chen et al., 2010; Barbot et al., 2012). Such laws express the dependence of frictional shear strength τ_f on the effective normal stress $\bar{\sigma}$, slip rate V (which we also call slip velocity), and evolving properties (state) of the contact population represented by the state variable θ, through:

$$\tau_f = \bar{\sigma} f = (\sigma - p)[f_o + a\ln(V/V_o) + b\ln(V_o\theta/L)],$$
$$\frac{\partial\theta}{\partial t} = 1 - \frac{V\theta}{L} \text{ or } \frac{\partial\theta}{\partial t} = -\frac{V\theta}{L}\ln\frac{V\theta}{L} \text{ or } \frac{\partial\theta}{\partial t} = \exp\left(-\frac{V}{V_c}\right) - \frac{V\theta}{L}\ln\frac{V\theta}{L}, \quad (1)$$

where σ is the normal traction, p is the pore pressure, f_o, V_o, a, b, and L are rate and state parameters, with L being the characteristic slip for state variable evolution, and V_c is the cut-off velocity of the order of 10^{-8} m/s. In these laws, the rate and state features result in small variations (of the order of 1-10%) from the baseline frictional strength given by $\bar{\sigma} f_o$. Despite being small, these variations are fundamentally important for physically and mathematically meaningful stability properties of frictional sliding (e.g., Rice, Lapusta, and Ranjith, 2001). In the steady state, $(a - b)$ is the rate-and-state parameter that can be used to model both stable, velocity-strengthening (VS) fault segments ($a - b > 0$) and potentially seismic, velocity-weakening (VW) fault segments ($a - b < 0$). Equations (1) give several proposed forms for the state variable evolution; which of these laws does a better job of representing the range of available experimental results and serves as the best simplified representation of the state variable evolution for simulations of long-term slip is an active area of research (Kato and Tullis, 2001; Hori et al., 2004; Rubin and Ampuero, 2005; Bayart et al., 2006; Ampuero and Rubin, 2008; Bhattacharya et al., 2015). We have used all of these forms in our modeling, and the obtained results are qualitatively, and often quantitatively, similar. We mostly use the aging form, since it incorporates the physically sound notion of friction increase in stationary contact, a feature required for the production of slip pulses (Perrin et al., 1995), and it is the easiest to properly resolve numerically. However, we have been working on verifying the robustness of the important results by using the other two forms of the state variable evolution.

The second emerging property of the earthquake source is additional substantial fault weakening at seismic slip rates. While theories of such dynamic weakening have a long history (Sibson, 1973), relatively recent laboratory confirmations of this phenomenon (Tsutsumi and Shimamoto, 1997; Tullis, 2007 and references therein) have put this notion on the earthquake science map. We have incorporated shear heating dynamic weakening mechanisms, such as flash heating and thermal pressurization, into our simulations, including those of repeating earthquakes (Lui and Lapusta, 2017). Dynamic weakening of creeping regions allows them to sustain seismic slip (Noda and Lapusta, 2010, 2013; Jiang and Lapusta, 2016, 2017). One shear-heating weakening mechanism with laboratory support is flash heating (e.g., Goldsby and Tullis, 2003, Beeler and Tullis, 2003, Rice, 2006, Beeler et al. 2008, Goldsby and Tullis, 2011), in which tips of contacting fault gouge grains heat up and weaken. Such weakening can be activated even for very small slips of the order of 10-100 microns if the shear strain rate is high enough. Another relevant mechanism is pore fluid pressurization (e.g., Sibson, 1973; Andrews, 2002; Bizzarri and Cocco, 2006a,b; Rice, 2006; Noda et al., 2009), in which rapid shearing raises the temperature and hence pore fluid pressure, lowering the effective normal stress and hence frictional resistance. To include flash heating and/or pore pressurization into our models, we modify the rate and state formulation (1) to

$$\tau_f = \bar{\sigma} f = (\sigma - p)\left[\frac{f_o - f_w + a\ln(V/V_o) + b\ln(V_o\theta/L)}{1 + L/\theta V_w} + f_w\right], \quad (2)$$

where V_w is the characteristic slip velocity at which flash heating starts to operate, f_w is the residual friction coefficient, and pore pressure p could be evolving due to shear heating as discussed below. Based

on laboratory experiments and flash heating theories, V_w is of the order of 0.1 m/s. Selecting much larger values of V_w than the seismic slip rates of the order of 1-10 m/s would effectively disable the additional weakening due to flash heating. The coupled temperature and pore pressure evolution is calculated by (Rice, 2006 and references therein, Noda et al., 2009, Noda and Lapusta, 2010):

$$\frac{\partial T}{\partial t} = \alpha_{th} \frac{\partial^2 T}{\partial y^2} + \frac{\omega(y)}{\rho c}, \quad \frac{\partial p}{\partial t} = \alpha_{hy} \frac{\partial^2 p}{\partial y^2} + \Lambda \frac{\partial T}{\partial t}, \tag{3}$$

where y is the space coordinate normal to the fault, T is the temperature, α_{th} and α_{th} are the thermal and hydraulic diffusivities, $\omega(y)$ is the heat generation rate the integral of which over the width w of the shearing layer equals to $\tau_f V$, ρc is the specific heat, Λ is pore pressure change per unit temperature change under undrained condition. (Note that this formulation can also include inelastic dilatancy, as an additional term in the equation for the pore pressure evolution.) The heat source, $\omega(y)$, is distributed in a narrow shear zone around the fault. The standard assumption is to take this term to represent the effect of uniform sliding in the fault zone of thickness w.

In our simulations, spontaneous long-term slip history of a fault governed by constitutive relations (1-5) and embedded into an elastic half-space is determined using the 3D simulation methodology of Lapusta and Liu (2009) and Noda and Lapusta (2010) developed with prior NSF and USGS support. The methodology incorporates slow tectonic-type loading and all dynamic effects of self-driven dynamic rupture. The algorithm allows us to treat accurately long deformation histories and to calculate, for each earthquake episode, initially quasi-static accelerating slip (nucleation process), the following dynamic rupture break-out and propagation, postseismic response, and ongoing slippage throughout the loading period in creeping fault region.

2. Improved models of the SF/LA repeaters and the surrounding creeping segment

As an important step towards creating realistic models that combine the Parkfield and creeping segment of the San Andreas fault and explore their interaction, including the possibility of dynamic rupture propagating through the creeping segment, we have been using the wealth of data on the SF and LA repeaters and their interaction to constrain friction properties of the creeping segment. The creeping segment contains a number of repeating earthquakes sequences, which are events with highly correlated seismograms that translate into similar moment magnitudes and nearly identical locations. Small repeating earthquakes occur on a number of other faults and their observations have been used to study various aspects of earthquake physics and mechanics (e.g., Ellsworth and Dietz, 1990; Vidale et al., 1994; Marone et al., 1995; Nadeau and Johnson, 1998; Schaff et al., 1998; Nadeau and McEvilly, 1999, 2004; Bürgmann et al., 2000; Beeler et al., 2001; Sammis and Rice, 2001; Igarashi et al., 2003; Imanishi et al., 2004; Nadeau et al., 2004; Schaff and Beroza, 2004; Matsubara et al., 2005; Allmann and Shearer, 2007; Chen et al., 2007; Rubinstein et al., 2012).

Many properties of these sequences have been successfully modeled as repeating ruptures of a VW patch embedded into a VS region (e.g., Chen and Lapusta, 2009; Lui and Lapusta, 2017; Figure 1). One of the most interesting observations about the repeaters is their scaling $T \sim M_0^{0.17}$ (Nadeau and Johnson, 1998) between the recurrence time T and seismic moment M_0, which is significantly different from $T \sim M_0^{1/3}$, the scaling that results in a simple conceptual model in which seismic events release all accumulated slip deficit $V_L T$ (where V_L is the long-term creeping velocity of the segment) and have stress drop independent of the seismic moment. Moreover, the recurrence time for the smallest repeaters is significantly longer than expected for moderate stress drops of 10 MPa, translating into stress drops of 3-4 GPa (3000-4000 MPa) for the simple model mentioned above (Nadeau and Johnson, 1998). Our models reproduce the observed scaling due to significant aseismic slip at the location of seismic events, with the fraction of aseismic slip being larger for smaller events. This makes sense based on stability studies of

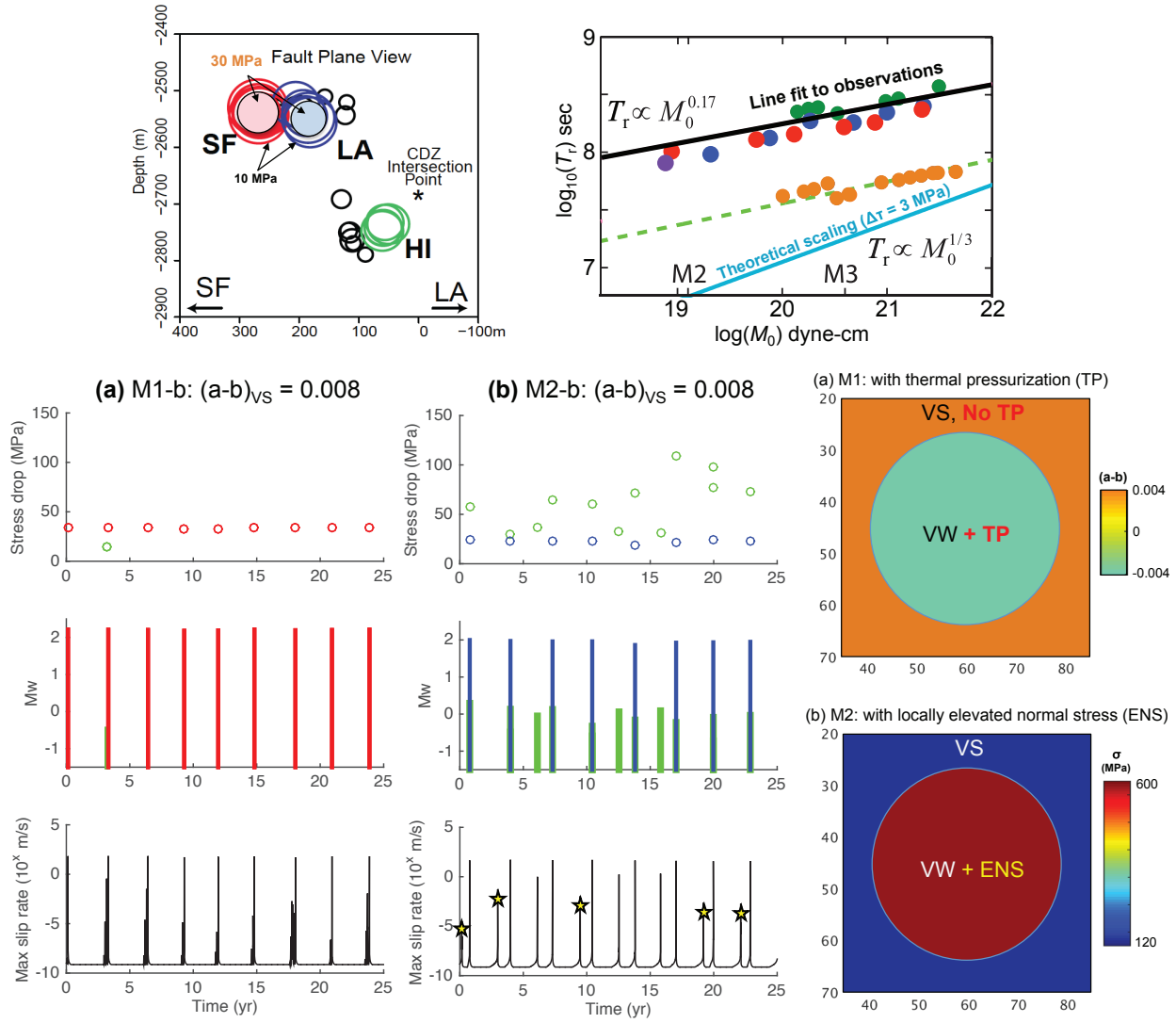

Figure 1: (Top left) Repeating earthquake sequences on the portion of the Parkfield segment of the San Andreas Fault (modified from Zoback et al., 2011). The SF and LA repeaters are spatially close to each other; source dimensions corresponding to 10 MPa stress drop (red and blue circles) would suggest that they are almost overlapping, while source dimensions based on 30 MPa stress drops (filled pink and light blue circles) as suggested by recent observations, indicate that they are separated in space, which explains why these are two separate, interacting repeating sequences. (Top right) The observed scaling $T \sim M_0^{0.17}$ (black line) between the recurrence time T and the seismic moment for all Parkfield repeaters has a different slope and much higher T than a standard theoretical scaling (blue line, see text). Our models of Parkfield repeaters explain the observed scaling by significant aseismic slip at the location of the repeaters; the results for repeaters on patches of different radii are shown for M1 (blue dots), M2 (red dots), and M3 (purple dots) as discussed below (Lui and Lapusta, 2017) as well as for the models of Chen & Lapusta (2009) (green and orange dots). (a-b) Models M1 with enhanced dynamic weakening in the VW patch and M2 with elevated normal stress in the VW patch, and the corresponding simulation results. Model M3 (not shown) combines some degree of enhanced dynamic weakening and elevated normal stress. Both models reproduce events of about Mw 2 and average stress drops of 25-30 MPa. Both models also have some variability in the moment and recurrence time of the events, more so in M2 which even has some much smaller, Mw ~0 events.

VW faults (Rice and Ruina, 1983; Rice et al., 2001; Rubin and Ampuero, 2005), since small enough VW patches would be below the nucleation size and hence completely aseismic. Our models confirm the idea of Beeler et al. (2001) that the observed scaling may be due to the presence of aseismic slip.

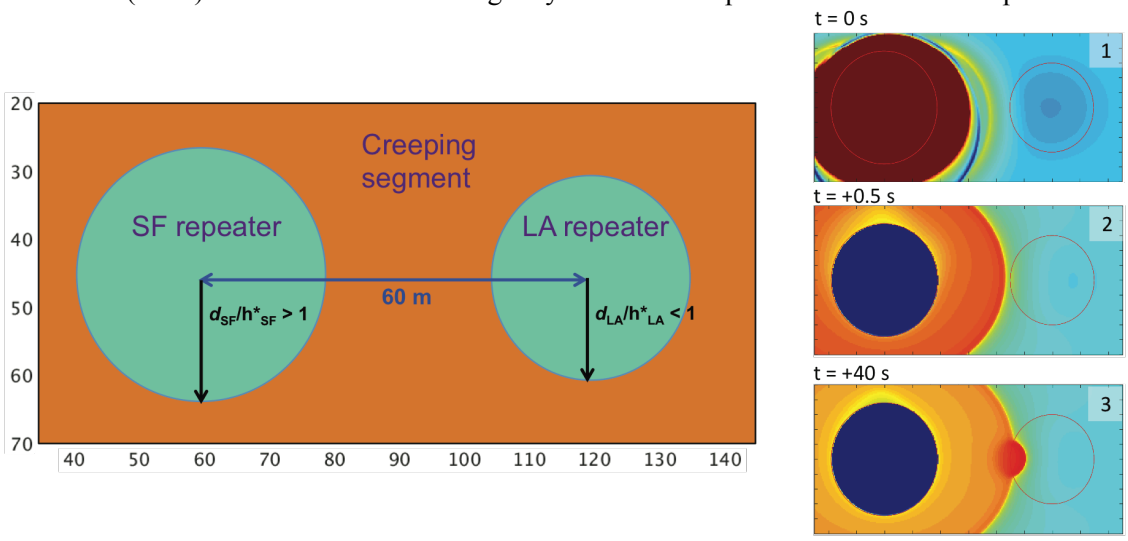

Figure 2: (Left) Model set up for simulating interaction of the SF and LA repeating sequences. The LA patch is slightly below the nucleation size such that it can only slip seismically with external stress perturbation. (Right) Example of a SF event triggering an LA event shown through snapshots of slip rate over the fault (red: seismic, yellow to orange: postseismic, blue: near plate rate). The SF patch ruptures at $t = 0$ s (panel 1), sending a postseismic creeping front to the neighboring LA patch (panels 2 and 3). The creeping front increases the shear stress on the LA patch (Lui and Lapusta, 2016) and triggers a seismic rupture there.

Our detailed modeling has been focused on the LA and SF repeaters, the main targets of the SAFOD experiment (Figure 1; Lui and Lapusta, 2016, 2017). These repeaters are characterized by two more interesting observations. The first one is their interaction before 2004 Parkfield event, with the LA events occurring within 24 hours of the SF events. The second is their relatively large stress drops, of 25-60 MPa on average, with local stress changes potentially as large as 90 MPa (Abercrombie, 1995, 2014; Nadeau and Johnson, 1998; Sammis et al., 1999; Dreger et al., 2007). We have created two types of models to reproduce the observations. In one type of models (M1 in Figure 1), the large stress drops are achieved by enhanced dynamic weakening due to thermal pressurization of pore fluids; with the narrowest shear zones and smallest hydraulic diffusivities cited in Rice (2006), the thermal pressurization is significant even for the Mw 2 events considered here. In the other type of models (M2 in Figure 1), a much elevated value of normal stress is assumed at the location of the repeaters, of ~600 MPa (e.g., due to a flattened "bump" on the slipping surface), with the weakening governed by the standard rate-and-state friction.

Both models can approximately reproduce relatively large average stress drops of ~30 MPa with local changes up to 80 MPa, along with the average moment and recurrence time, as well as the interaction between two sequences, with LA events occurring tens of seconds to hours after the SF ones. The interaction occurs mainly due to the effect of postseismic slip between the two patches (Lui and Lapusta, 2016, 2017; Figure 2). Matching the interaction time to minutes/hours has allowed us to constrain the VS properties of the creeping region between the repeaters. For the assumed properties of the VW patches that match the repeaters reasonably well and effective normal stress of 120 MPa assumed based on SAFOD inferences, our modeling suggests that the VS region has the rate-and-state property $(a - b)$ in the range of 0.004 to 0.008. This is consistent with other studies in the area (Barbot, 2009; Chang, 2013) as well as laboratory experiments.

Significantly, both models of the kind M1 and M2 are capable of reproducing the observed atypical T_r-M_o scaling relation (Figure 1, top right). We vary the patch size to obtain repeating events ranging from $M_w \sim 2$ to 4 (blue and red dots in the Figure). Note that V_{pl} = 23 mm/yr in our models. We find that both models reproduce not only the observed scaling but also the absolute values of the recurrence times. This is because our events have stress drops around 25 to 35 MPa, ~4-5 times higher than those in Chen (2009). That is why they occur less frequently even for loading rate of 23 mm/yr, something the standard rate-and-state modeling of Chen (2009) could not achieve. However, the underlying reason for matching the scaling exponent is the same as in Chen (2009), which is the presence of significant aseismic slip on the patches, the fraction of which decreases as the patch, and hence patch-to-h* ratio, increases. Therefore, one can reproduce the observed scaling in two ways: (1) larger stress drops of ~30 MPa and inferred large-scale creeping rate of V_{pl} = 23 mm/yr as in our models M1-M2, or (2) more typical stress drops of ~7 MPa based on standard rate-and-state friction and smaller, at least locally, surrounding creeping rate of 4.5 mm/yr as in Chen (2009).

Observations show that even repeating events are not identical, with significant differences in seismic moment and recurrence time. For example, the average recurrence time *T* of the seven SF events before year 2004 is 2.9 years, with a standard deviation of 0.35 years. Furthermore, the repeating events are neither time-predictable nor slip-predictable (Rubinstein et al, 2012), which basically means, counter intuitively, that smaller recurrence intervals often follow larger events and that smaller events often follow larger recurrence intervals,

We find that some of this variability can be explained by complex slip dynamics in our models (Figure 3) with relatively simple distributions of friction properties, uniform within the VW and VS areas. For example, the interseismic period between repeaters E1 and E3 in Figure 3 is among the longest ones in that simulation, and yet the magnitude of E3 is among the smallest. Such counterintuitive observation occurs in our model because of an aseismic transient between the events that culminates in a tiny event E3; the transient releases enough stress on the patch to both elongate the recurrence time and result in a somewhat smaller repeater afterwards.

At the same time, the presence of many repeating sequences in the creeping segment suggests that the friction properties in the area may be heterogeneous in general, with potentially smaller VW patches that remain aseismic (being smaller than the nucleation size) or produce much smaller seismic events but perturb the surrounding creep. Furthermore, the distribution of the VS properties can also be heterogeneous, given unsteady creep observed or inferred on the creeping segment (Schulz, 1989; Gladwin et al., 1994; Nadeau and McEvilly, 2004; Maurer and Johnson, 2014). We have started to explore the effects of VW/VS property distributions in terms of the resulting slip patterns, effects on nucleation, etc (ongoing work with Natalie Higgins and Kavya Sudhir), including simple patterns of properties as well as more complex distributions motivated by truncated random fields (e.g., Mai and Beroza, 2002, Brodsky et al., 2011).

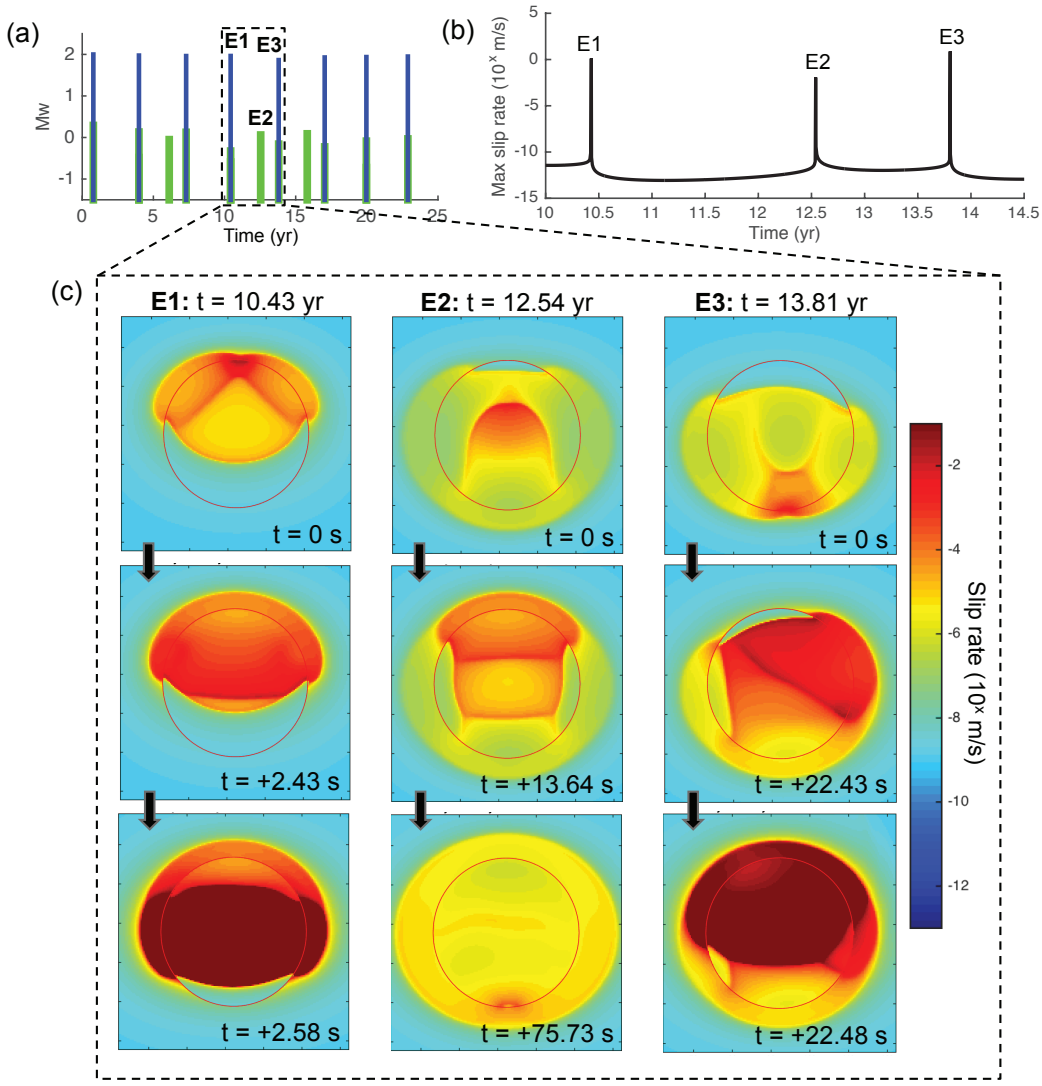

Figure 3: Longer interseismic period resulting in a smaller repeater due to interseismic stress release. (a) M_w of the events in M2-b (Fig. 1), showing the repeating sequence (blue, including E1 and E3) and much smaller seismic events (green, including E2). The interseismic period is longer when additional events occur on the patch. (b) Slip velocity at the center of the VW patch between 10 to 14.5 years. (c) Snapshots of slip velocity on and around the VW patch (red open circle) during events E1-E3. E2 starts as a small seismic event that sends an aseismic slip transient through the entire patch and releases shear stress during the process. This mostly aseismic release of stress explains both the longer interseismic period before E1 and the fact E3 is smaller than E1 by ~30%.

3. Connecting depth limits of interseismic locking, microseismicity, and large earthquakes on mature strike-slip faults such as SAF

Our modeling related to the areas of Mw 7.6 1999 Chi-Chi earthquake and Mw 9.0 2011 Tohoku-Oki earthquake revealed that earthquake rupture may break through large portions of creeping segments, due to co-seismic weakening such as the thermal pressurization of pore fluids discussed in section 1 (Noda and Lapusta, 2013). The possibility that creeping segments - currently perceived as barriers – may

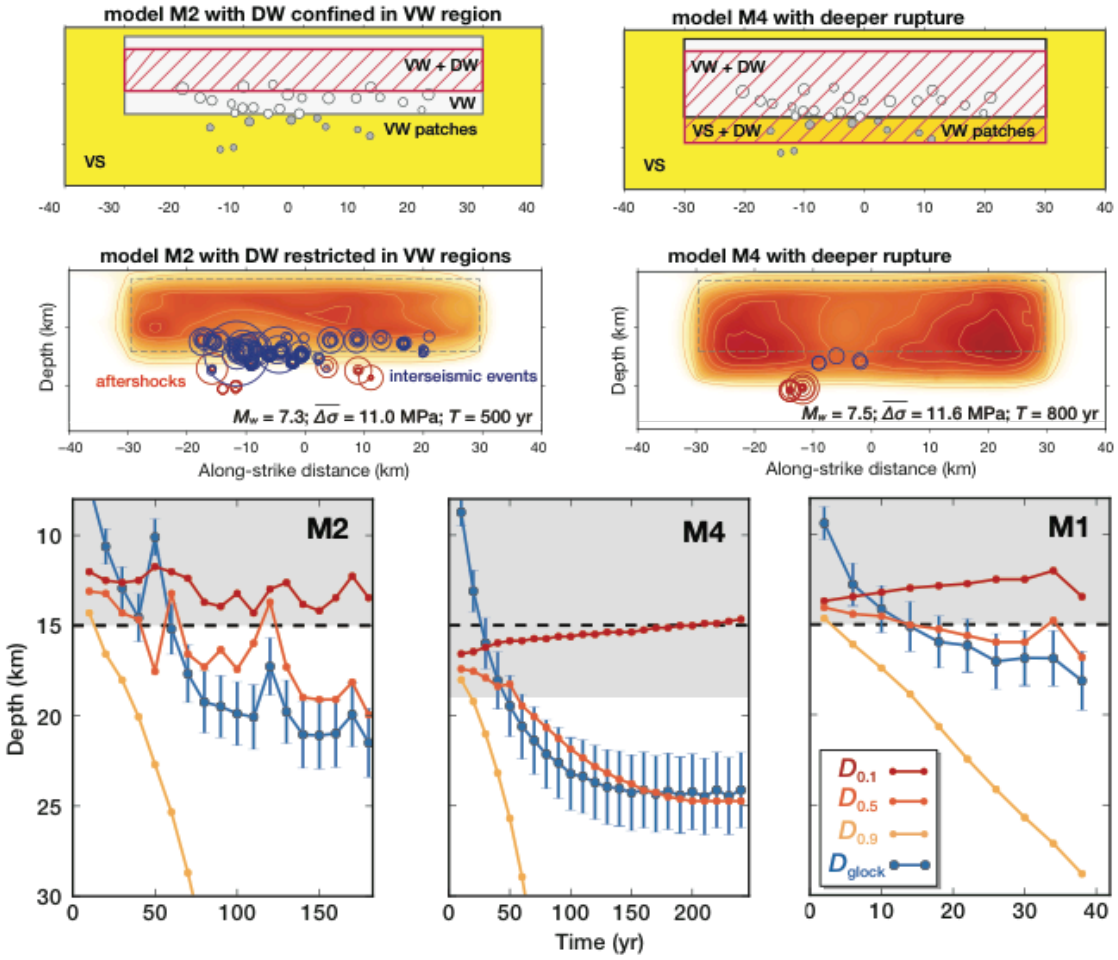

Figure 4: Connecting the depth limits of interseismic locking, microseismicity, and large earthquakes in models of long-term fault slip (modified from Jiang and Lapusta, 2016; 2017). (Top panels) Examples of fault models which incorporate depth-variable friction properties. In both cases, the low-velocity rate-and-state properties are the same, with velocity-weakening (VW) region (white) embedded into velocity-strengthening areas (yellow). However, the extent of dynamic weakening (DW, red lines) that occurs co-seismically differs, being limited to the VW region in one model (M2, left) and extending deeper into the VS area in the other (M4, right). (Middle panels) The associated coseismic slip distribution during a typical large event (red color scale) and microseismicity before the event (blue circles) and after the event (red circles). The microseismicity is suppressed for the model with deeper slip penetration. (Bottom panels) Evolution of the locked-creeping transition in the two models (M2 and M4), as well as in the third model (M1) which has no DW. The depths $D_{0.1}$, $D_{0.5}$, and $D_{0.9}$, at which slip rates reach 0.1 V_{pl}, 0.5 V_{pl}, and 0.9 V_{pl}, respectively, where V_{pl} is the loading rate, are shown in red, orange, and yellow. The corresponding geodetic locking depth D_{glock}, estimated from interseismic surface velocity using a 2-D elastic dislocation model and typical data uncertanties, is shown in blue. The black dashed line corresponds to the VW/VS transition. $D_{0.1}$ corresponds to the microseismicity-promoting front; note that it is mostly below the VW region in M4, suppressing microseismicity. $D_{0.1}$ and $D_{0.9}$ diverge toward the late interseismic period, due to the shrinkage of the effectively locked zone and the expansion of the slip deficit zone. D_{glock} approximately corresponds to $D_{0.5}$, deepens with time, and bounds the depth limit and potency release of large earthquakes in our models.

generate large seismic slip and hence significantly enlarge the size of the expected event, as may have occurred in the Mw 9.0 2011 Tohoku-Oki earthquakes, requires re-evaluation of seismic hazard in many areas, including California.

We have successfully applied this paradigm to exploring the possibility of deeper slip in large earthquakes on the SAF (Figure 6). It is typically assumed that all seismic slip is confined within the seismogenic zone - often defined by the extent of the background seismicity or geodetically determined locking depth - with regions below creeping. Fault models based on standard rate-and-state laws support such assumptions, interpreting the locked zones as areas of VW properties that allow for earthquake nucleation, and the deeper creeping fault extensions as areas of VS properties that inhibit earthquake slip. However, enhanced co-seismic weakening of fault friction could be active not only in the VW part of the fault but also in the deeper VS fault extensions. As earthquake rupture penetrates into the creeping fault areas, it significantly increases slip rates there, potentially activating the co-seismic weakening and turning the stable fault areas into seismogenic ones. Recent observational studies have suggested that earthquake rupture could penetrate into the deeper creeping regions (Shaw and Wesnousky, 2008), and yet deep slip is difficult to detect due to limited resolution of source inversions with depth.

We have developed models of faults with different depth-dependent friction properties around the bottom of the seismogenic zone to explore the relation between the depths of microseismicity, interseismic fault locking, and large earthquakes. Our simulations show that earthquakes indeed can penetrate into the deeper creeping fault extension, enabled by enhanced dynamic weakening at high slip rates. Depending on how deep coseismic slip reaches, the microseismicity at depth could be eliminated in most or all of the interseismic period due to the stress concentration front being located below the low-rate VW zone that can nucleate small events (Jiang and Lapusta, 2016; Figure 6). Parts of the deeper creeping region that experienced coseismic slip and hence stress drop are locked right after a seismic event but start creeping relatively soon, resulting in the time-dependent decrease of locking depth with time. As a consequence, the locked-creeping transition zone can occur over a broad depth range. The extent of the zone and its evolution can be quantified by tracking the depths $D_{0.1}$, $D_{0.5}$, and $D_{0.9}$, at which slip rates reach 0.1 V_{pl}, 0.5 V_{pl}, and 0.9 V_{pl}, respectively, where V_{pl} is the loading rate (Jiang and Lapusta, 2017; Figure 6). $D_{0.1}$ corresponds to the effective locking depth D_{elock} which is associated with microseismicity due to concentrated loading. The geodetic locking depth D_{glock}, estimated from interseismic surface velocity using a 2-D elastic dislocation model, approximately corresponds to the location of $D_{0.5}$, which can be explained by theoretical reasoning (Jiang and Lapusta, 2017).

We find the divergence of the two depths, depth D_{elock} and D_{glock}, diverge toward the late interseismic period, due to the shrinkage of the effectively locked zone and the expansion of the slip deficit zone. This divergence reflects the extent of deeper coseismic rupture and/or postseismic slip. Our model predictions are consistent with the available seismic and geodetic observations of the Carrizo and Coachella segments on the San Andreas fault, where the depth of microseismicity is shallower than the geodetically estimated locking depth.

The effective locking depth $D_{elock} = D_{0.1}$ (by our definition) corresponds to higher stressing rates than the ones shallower, due to the creep in the neighboring transition zone, and hence it is relevant to microseismicity at transitional depths (Fig. 5). In the interseismic period, the upper extent of the microseismicity approximately corresponds to the effective locking depth D_{elock} (Fig. 5) even though there are nucleation-promoting patches shallower in our model. This is because D_{elock} marks the top of the locked-creeping transition zone, throughout which the fault creep rates vary and concentrated stressing arises. If the enhanced stressing is located within the VW fault areas, as in models M1-M3, microseismicity is promoted, in particular, at locations of fault heterogeneity. Such considerations are supported by the strong correlation between the decreasing D_{elock} and shallower seismicity in M1 as well as the near-constant depth of both in M2 and M3. Model M4 demonstrates that when D_{elock} is deeper than the VW/VS transition, microseismicity is largely absent, occurring mostly on deeper patches positioned for generality.

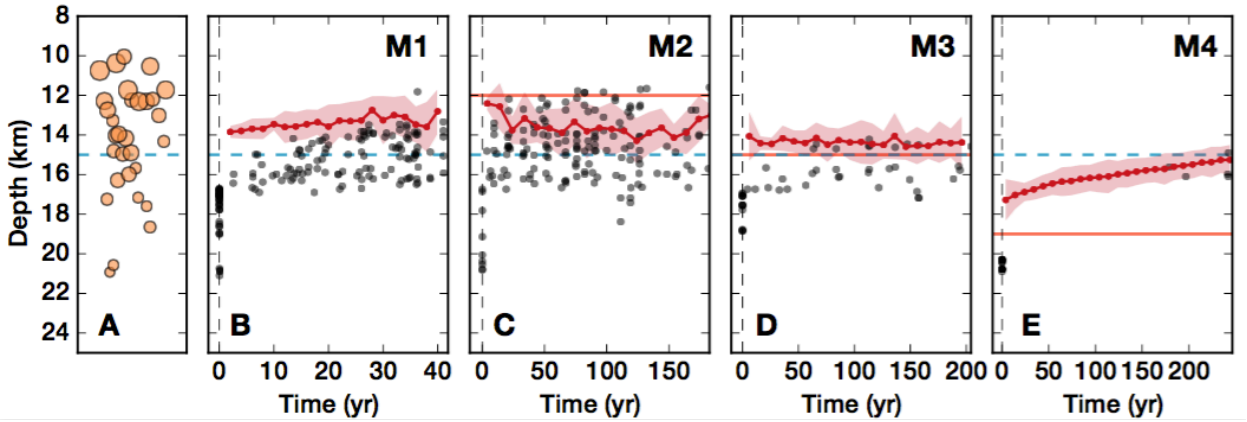

Figure 5: Time evolution of the effective locking depth, $D_{0.1}$, and microseismicity in our models. (A) The depth distribution of the nucleation-prone VW patches that promote microseismicity. The horizontal spacing between patches is arbitrarily scaled to focus on the depth. (B–D) The evolution of $D_{0.1}$ (red dotted lines and red-colored areas) and microseismicity (grey dots) in M1–M4. $D_{0.1}$ is estimated for the along-strike interval of x = [-20, 20] km, with red dotted lines indicating the mean values of $D_{0.1}$ and red-colored areas indicating the one-standard-deviation range over the along-strike interval. The VW/VS boundary and depth limit of DW are denoted by the blue dashed and orange horizontal lines, respectively. Note that $D_{0.1}$ corresponds well to the upper extent of the microseismicity and its evolution.

When D_{elock} is above the VW/VS transition, most of the microseismicity occurs in or right next to the band between the (shallower) D_{elock} and (deeper) VW/VS transition. Hence the microseismicity forms a prominent and relatively narrow band, the width of which approximately corresponds to the large-scale nucleation size h^* and the depth of which corresponds to the bottom cutoff of microseismicity D_{seis}, since not many seismic events can occur spontaneously in the deeper VS fault extensions. If the band does not exist, i.e. D_{elock} is deeper than the VW/VS transition, then there is no pronounced microseismicity at the transition (M4) (Jiang and Lapusta 2016).

In the postseismic periods of all four models, deeper aftershocks (i.e., between 18 and 21 km depth) appear for a limited time following large earthquake ruptures. These aftershocks occur on patches that do not produce seismicity in the interseismic period, because their sizes are chosen to be below the quasi-static estimate of the nucleation size. Nucleation of these aftershocks on the VW patches of subcritical sizes is made possible by the accelerated postseismic fault slip rates, indicating that the nucleation size depends on the loading rates, as was noted in earlier studies (Kaneko and Lapusta, 2008). Note that such transient deep aftershocks have been observed after a number of large earthquakes (Doser and Kanamori, 1986; Schaff et al., 2002; Rolandone et al., 2004; Jiang and Lapusta, 2016).

We find that the depth extent of large earthquake ruptures, D_{rupt}, is shallower than the geodetically estimated locking depth D_{glock} in the late interseismic period (Figure 6) and the closely related $D_{0.5}$. Such a relation can be explained from fault-slip partitioning with depth. Given the quasi-periodic nature of large earthquakes in our models, long-term fault slip at the plate rate is approximately balanced by the combination of co-, post-, and inter-seismic slip for each cycle (i.e., each large seismic event and the following post- and inter-seismic period). If, around the depth of D_{rupt} and shallower, much of the slip budget is accommodated by coseismic and postseismic slip, as occurs in our models, then not much is left for interseismic slip, and hence D_{glock}, which represent the combined effect of the entire interseismic transition zone, tends to be deeper than D_{rupt}. In the extreme case with no postseismic slip, D_{rupt} would be deeper than D_{glock}, since the fault regions below D_{rupt} would have to slip with the long-term slip rate V_{pl} and any interseismic slip penetrating up, into the seismically ruptured domain, would make D_{glock} shallower than D_{glock}. In our scenarios with significant postseismic slip, the geodetic locking depth D_{glock}

in the late interseismic period is at or below the rupture depth D_{rupt}. We have also considered cases with much smaller postseismic slip; D_{rupt} and D_{glock} are nearly the same in those cases as well.

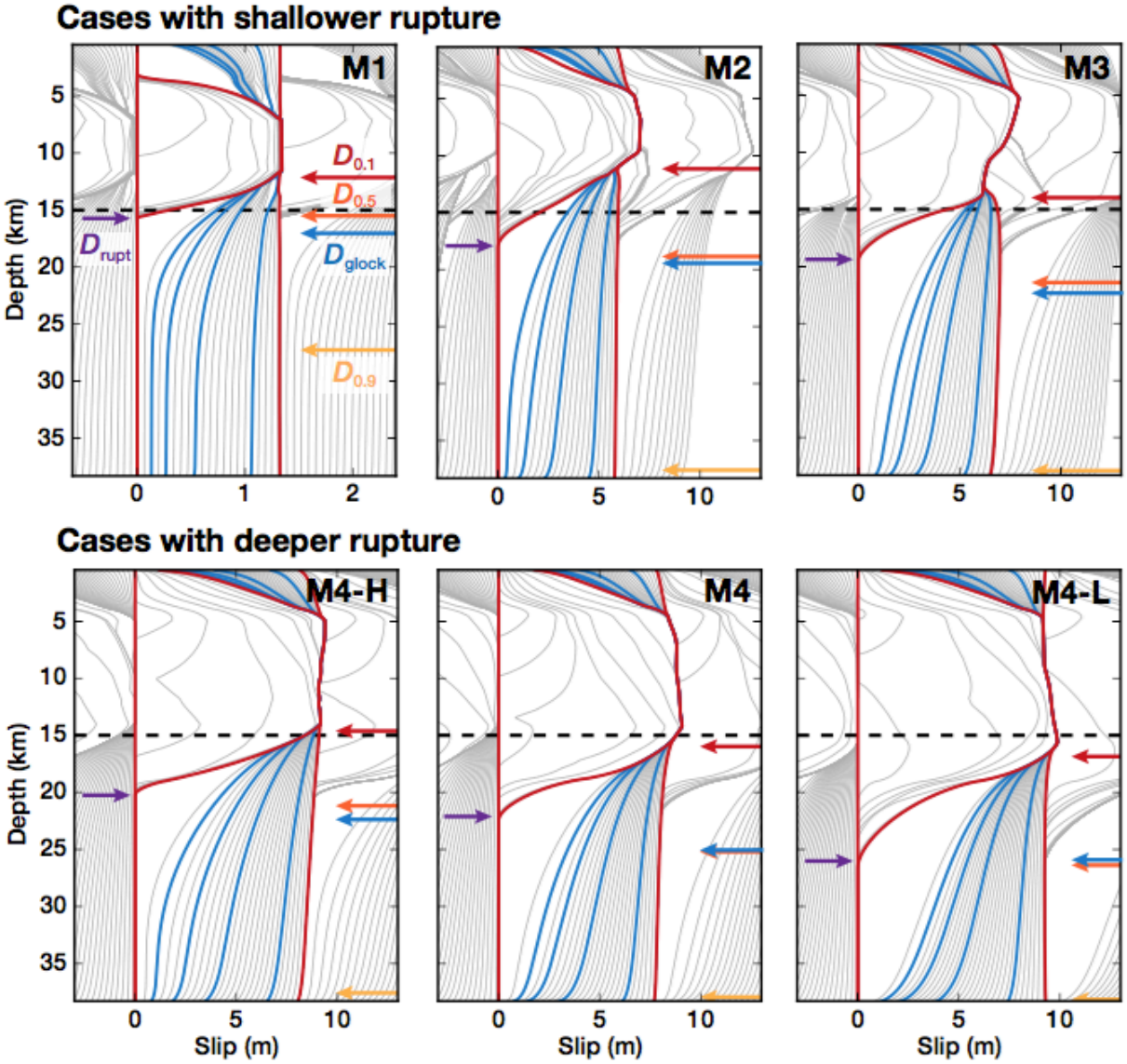

Figure 6: The slip budget during a seismic cycle is highlighted along a depth profile located at 7 km along the strike, with a coseismic period outlined by red lines and the ensuing post- and inter-seismic period indicated by five representative times in blue ($0.1T$, $0.2T$, $0.4T$, $0.8T$ and T from left to right, where T is the earthquake recurrence interval). The cumulative fault slip (gray lines) is plotted for the coseismic period with intervals of 0.5 s (M1) and 1 s (the other models) and for aseismic periods with intervals of 2 yr (M1) and 10 yr (the other models). Depths $D_{0.1}$, $D_{0.5}$, and $D_{0.9}$ are estimated for a late interseismic period ($0.8T$) and indicated by red, orange, and yellow arrows, respectively. The geodetic locking depth, D_{glock} estimated for a 10-yr time period centered around $0.8T$, is indicated by the blue arrow. The depth extent of large earthquake rupture, D_{rupt}, is indicated by the purple arrow. The cumulative fault slip is offset by the total slip prior to the large event. The low-velocity VW/VS boundary is marked by the black dashed line.

Therefore, for a range of models, D_{glock} in the late interseismic period provides an upper bound on the depth of large earthquakes, making it relevant to seismic hazard. How reliable this bound would be in

practice depends on the accuracy of D_{glock}, which is susceptible to strong trade-offs with the long-term fault slip rate and quite sensitive to model assumptions.

4. Understanding the seismological observables from our seismic sources

We have developed a capability of computing synthetic seismograms for small events produced in our models (Lin and Lapusta, 2016), starting with far-field expressions based on elastic Green's functions (e.g., Aki and Richards, 2002; Kaneko and Shearer, 2014, 2015). We plan to eventually incorporate attenuation and noise. The synthetic seismograms can be used to determine seismological observables for repeating earthquakes produced in our models, including event durations, source sizes, and stress drops, in the same way as it is done for natural events (e.g., Madariaga, 1967; Brune, 1970, 1971; Sato and Hirasawa, 1973; Kanamori and Anderson, 1975; Ide and Beroza, 2001; Allmann and Shearer, 2009; Baltay et al, 2011; Hauksson et al, 2012; Abercrombie, 2014; Figure 7). This will enable us to determine how well the seismologically estimated quantities correspond to the actual source properties that are fully known for our dynamic sources. Such comparison studies for some simple dynamic source models showed potential large discrepancies (Kaneko and Shearer, 2014, 2015) confirmed by our preliminary studies of generic sources. In particular, we would like to examine whether the large average stress drops that we obtain in our source models of the SF and LA repeaters would be correctly estimated from synthetic seismograms, and determine the most realistic sources in our models by comparison of our synthetic seismograms with the observed ones.

We have also investigated whether dynamic weakening used in our models is consistent with the observation of magnitude-independent stress drops. At first glance, these two observations seem incompatible. Larger events may experience greater weakening and should thus have lower final stresses, leading to an increase in stress drop with event size. However, our results show that models with dynamic weakening can produce magnitude-invariant stress drops for a range of event sizes. This is due to larger events having lower average prestress when compared to smaller events. The additional weakening would allow the final stresses to also be lower, but the stress drops remain invariant. We observe larger initial stresses for smaller events as compared to medium-sized events, and we get roughly constant stress drops for events spanning up to five orders of magnitude in moment (Perry and Lapusta, 2016).

REFERENCES

Abercrombie, R. E., Earthquake source scaling relationships from− 1 to 5 ML using seismograms recorded at 2.5 km depth, *J. Geophys. Res*., **100** (B12), 24015-24036, 1995.

Abercrombie, R. E., Stress drops of repeating earthquakes on the San Andreas Fault at Parkfield, *Geophys. Res. Lett.*, **41**, doi: 10.1002/2014GL062079, 2014.

Aki, Keiiti, and Paul G. Richards. *Quantitative seismology*. Vol. 1. 2002.

Allmann, B. P., and P. M. Shearer, Spatial and temporal stress drop variations in small earthquakes near Parkfield, California, *J. Geophys. Res*., **112**, B04305, doi:10.1029/2006JB004395, 2007.

Allmann, B. P., and P. M. Shearer, Global variations of stress drop for moderate to large earthquakes. *J. Geophys. Res*., **114**(B1), B01310, doi:10.1029/2008JB005821, 2009.

Ampuero, J.-P., and A. M. Rubin, Earthquake nucleation on rate and state faults-Aging and slip laws, *J. Geophys. Res.*, **113**, B01302, doi:10.1029/2007JB005082, 2008.

Andrews, D. J., A fault constitutive relation accounting for thermal pressurization of pore fluid, *J. Geophys. Res*., **107**(B12), 2363, doi:10.1029/2002JB001942, 2002.

Baltay, A., S. Ide, G. Prieto, and G. Beroza, Variability in earthquake stress drop and apparent stress. *Geophys. Res. Lett.*, **38**(6)., 2011.

Barbot, S., Y. Fialko, and Y. Bock (2009), Postseismic deformation due to the M_W 6.0 2004 Parkfield earthquake: Stress-driven creep on a fault with spatially variable rate- and-state friction parameters, *Journal of Geophysical Research: Solid Earth*, *114*(B7), doi:10.1029/2008JB005748, b07405.

Barbot, S., N. Lapusta, and J.-P. Avouac, Under the hood of the earthquake machine: Toward predictive modeling of the seismic cycle, *Science*, *336*(6082), 707–710, doi:10.1126/science.1218796, 2012.

Bayart, E., A. M. Rubin, and C. Marone, Evolution of Fault Friction Following Large Velocity Jumps, *Eos Trans. AGU*, **87**(52), Fall Meet. Suppl., S31A-0180, 2006.

Beeler, N. M., T. E. Tullis, and J. D. Weeks , The roles of time and displacement in the evolution effect in rock friction, *Geophys. Res. Lett*., **21**, 1987–1990, 1994.

Beeler, N. M., D. L. Lockner, and S. H. Hickman, A simple stick-slip and creep-slip model for repeating earthquakes and its implication for microearthquakes at Parkfield, *Bull. Seismol. Soc. Am*., **91**, 1797–1804, 2001.

Beeler, N. M., and T. E. Tullis, Constitutive relationships for fault strength due to flash-heating. In: *2003 SCEC Annual Meeting Proceedings and Abstracts*, vol. 13, p. 66. Los, Angeles: Southern California Earthquake Center, Univ. of Southern California, 2003.

Beeler, N. M., T. E. Tullis, and D. L. Goldsby , Constitutive relationships and physical basis of fault strength due to flash-heating, *J. Geophys. Res*., **113**, B01401, doi:10.1029/2007JB004988, 2008.

Bhattacharya, P., Rubin, A. M., Bayart, E., Savage, H. M., & Marone, C., Critical evaluation of state evolution laws in rate and state friction: Fitting large velocity steps in simulated fault gouge with time-, slip-, and stress-dependent constitutive laws. *J. Geophys. Res.*, **120,** 9, 6365-6385, 2015.

Bizzarri, A., and M. Cocco, A thermal pressurization model for the spontaneous dynamic rupture propagation on a three-dimensional fault: 1. Methodological approach, *J. Geophys. Res*., **111**, B05303, doi:10.1029/2005JB003862, 2006a.

Bizzarri, A., and M. Cocco, A thermal pressurization model for the spontaneous dynamic rupture propagation on a three-dimensional fault: 2. Traction evolution and dynamic parameters, *J. Geophys. Res*., **111**, B05304, doi:10.1029/2005JB003864, 2006b.

Blanpied, M. L., D. A. Lockner and J. D. Byerlee, Fault stability inferred from granite sliding experiments at hydrothermal conditions, *Geophys. Res. Letters*, **18** (4), 609-612, 1991.

Blanpied, M. L., D. A. Lockner and J. D. Byerlee, Frictional slip of granite at hydrothermal conditions, *J. Geophys. Res*., **100**, 13045-13064, 1995.

Brodsky, E. E., J.J. Gilchrist, A. Sagy, C. Collettini, Faults smooth gradually as a function of slip, *Earth and Planetary Science Letters,* 302, 185-193, 2011.

Brune, J., Tectonic stress and the spectra of seismic shear waves from earthquakes, *J. Geophys. Res.*, **75**, 4997–5009, doi:10.1029/JB075i026p04997, 1970.

Brune, J. N., Correction, *J. Geophys. Res.*, **76**, 5002, 1971.

Bürgmann, R., D. Schmidt, R. M. Nadeau, M. d'Alessio, E. Fielding, D. Manaker, T. V. McEvilly, and M. H. Murray, Earthquake potential along the northern Hayward fault, California, *Science*, **289**, 1178–1182, 2000.

Chang, S.-H., J.-P. Avouac, S. Barbot, and J.-C. Lee (2013), Spatially variable fault fric- tion derived from dynamic modeling of aseismic afterslip due to the 2004 Parkfield earthquake, *Journal of Geophysical Research: Solid Earth*, *118*(7), 3431–3447, doi: 10.1002/jgrb.50231..

Chen, K. H., Bürgmann, R., and Nadeau, R. M., Do repeating earthquakes talk to each other?, *EOS Trans. AGU*, S33C-1469, 2007.

Chen, T., and N. Lapusta , Scaling of small repeating earthquakes explained by interaction of seismic and aseismic slip in a rate and state fault model, *J. Geophys. Res.*, 114, B01311, doi:10.1029/2008JB005749, 2009.

Chen, T., and N. Lapusta, Interaction of small repeating earthquakes in a rate and state fault model, *AGU Fall Meeting*, T33B-2255, 2010.

Dieterich, J. H., Modeling of rock friction- 1 Experimental results and constitutive equations, *J. Geophys. Res.*, **84**, 2161-2168, 1979.

Dieterich, J. H., Constitutive properties of faults with simulated gouge, in *Mech. Beh. Crustal Rocks*, Geophys. Monogr. Ser., **24**, ed. by N. L. Carter, M. Friedman, J. M. Logan and D. W. Stearns, AGU, Washington, DC, 103-120, 1981.

Dieterich, J. H. Applications of rate- and state-dependent friction to models of fault slip and earthquake occurrence. In Kanamori, H. (ed.) *Treatise on Geophysics*, **4**, chap. 4, 107–129 (Elsevier, Amsterdam, 2007).

Doser, D. I., and H. Kanamori (1986), Depth of seismicity in the Imperial Valley region (1977-1983) and its relationship to heat flow, crustal structure, and the October 15, 1979, earthquake, *J. Geophys. Res.*, *91,* 675-688.

Dreger, D., R. M. Nadeau, and A. Chung, Repeating earthquake finite source models: Strong asperities revealed on the San Andreas Fault. *Geophys. Res. Lett.*, **34**(23), L23302, doi:10.1029/2007GL031353 2007.

Ellsworth, W. L. and L. D. Dietz, Repeating earthquakes: characteristics and implications, Proc. of Workshop 46, the 7th U.S.-Japan Seminar on Earthquake prediction, U.S.Geol.Surv. Open-File Rept. 90-98, 226-245, 1990.

Gladwin, M. T., R. L. Gwyther, R. H. G. Hart, and K. S. Breckenbridge, Measurements of the Strain Field Associated with Episodic Creep Events on the San Andreas Fault at San Juan Bautista, California, *Journal of Geophysical Research*, 99, 4559-4565, 1994.

Goldsby, D. L., and T. E. Tullis, Flash heating/melting phenomena for crustal rocks at (nearly) seismic slip rates. In: *2003 SCEC Annual Meeting Proceedings and Abstracts*, vol. 13, p. 98-99. Los Angeles: Southern California Earthquake Center, Univ. of Southern California, 2003.

Goldsby, D. L. and T. E. Tullis, Flash heating leads to low frictional strength of crustal rocks at earthquake slip rates, *Science*, **334**, 216-218, DOI: 10.1126/science.1207902, 2011.

Hauksson, E., W. Yang, and P. M. Shearer, Waveform Relocated Earthquake Cat- alog for Southern California (1981 to June 2011), *Bull. Seis. Soc. Amer.*, *102*(5), 2239– 2244, 2012.

Hori, T., N. Kato, K. Hirahara, T. Bada, and Y. Kaneda, A numerical simulation of earthquake cycles along the Nankai trough, southwest Japan: Lateral variation in frictional property due to slab geometry controls the nucleation position, *Earth. Planet. Sci. Lett.*, 228, 215-226, 2004.

Ide, S., and G. C. Beroza, Does apparent stress vary with earthquake size. *Geophys. Res. Lett.,* **28**(17), 3349-3352, 2001.

Igarashi, T., Matsuzawa, T., and A. Hasegawa, Repeating earthquakes and interplate aseismic slip in the northeastern Japan subduction zone, *J. Geophys. Res.* 108, B5, 2249, 2003.

Imanishi, K., W. L. Ellsworth, S. G. Prejean, Earthquake source parameters determined by the SAFOD Pilot Hole seismic array, *Geophys. Res. Letters*, **31**, L12S09, doi:10.1029/2004GL019420, 2004.

Jiang, J., and N. Lapusta, Deeper penetration of large earthquakes on seismically quiescent faults, *Science*, 352, 2016.

Kanamori, H., & Anderson, D. L. Theoretical basis of some empirical relations in seismology. *Bull. Seismol. Soc. Am.*, **65** (5), 1073-1095, 1975.

Kaneko, Y., and N. Lapusta (2008), Variability of earthquake nucleation in continuum models of rate-and-state faults and implications for aftershock rates, *J. Geophys. Res. Solid Earth*, *113*(B12), B12,312, doi:10.1029/2007JB005154.

Kaneko, Y., and P. M. Shearer, Seismic source spectra and estimated stress drop derived from cohesive-zone models of circular subshear rupture. *Geophys. J. Int.*, **197**, 1002-1015, 2014.

Kaneko, Y., and P. M. Shearer, Variability of seismic source spectra, estimated stress drop, and radiated energy, derived from cohesive zone models of symmetrical and asymmetrical circular and elliptical ruptures. *J. Geophys. Res*, **120**(2), 1053-1079, 2015.

Kato, N., and T. E. Tullis, A composite rate- and state-dependent law for rock friction, *Geophys. Res. Lett.*, 28, 1103–1106, 2001.

Lapusta, N., and Y. Liu, 3D boundary-integral modeling of spontaneous earthquake sequences and aseismic slip, accepted for publication, *J. Geophys. Res.*, 2009.

Madariaga, R., Dynamics of an expanding circular crack, *Bull. Seismol. Soc. Am.*, **66**, 639–666, 1976.
Mai, P. M., & Beroza, G. C. A spatial random field model to characterize complexity in earthquake slip. *J. Geophys. Res.*, **107** (B11), 2002.
Marone, C., Vidale, J. E., and W. L. Ellsworth, Fault healing inferred from time-dependent variations in-source properties of repeating earthquakes, *Geophys. Res. Lett.,* 22, 3095-3098, 1995.
Marone, C. , Laboratory-derived friction laws and their application to seismic faulting, Ann. *Rev. Earth Planet. Sci*., **26**, 643– 696, 1998.
Matsubara, M., Y. Yagi, and K. Obara, Plate boundary slip associated with the 2003 off-Tokachi earthquake based on small repeating earthquake data, *Geophys. Res. Lett*., **32**, L08316, doi:10.1029/2004GL022310, 2005.
Maurer, J., and K. M. Johnson, Fault coupling and potential for earthquakes on the creeping section of the Central San Andreas Fault, *J. Geophys. Res*., 119, 4414-4428, 2014.
Nadeau, R. M., and L. R. Johnson, Seismological studies at Parkfield VI: Moment release rates and estimates of source parameters for small repeating earthquakes, *Bull. Seism. Soc. Am.,* 88, 1998.
Nadeau, R. M., and T. V. McEvilly, Fault slip rates at depth from recurrence intervals of repeating microearthquakes, *Science*, **285**, 718–721, 1999.
Nadeau, R. M., and T, V. McEvilly, Periodic Pulsing of Characteristic Microearthquakes on the San Andreas Fault, *Science*, 303, 220-223, 2004.
Nadeau, R. M., A. Michelini, R. A. Uhrhammer, D. Dolenc, T. V. McEvilly, Detailed kinematics, structure and recurrence of micro-seismicity in the SAFOD target region, *Geophys. Res. Letters*, **31**, L12S08, doi:10.1029/2003GL019409, 2004.
Noda, H., E. M. Dunham, and J. R. Rice, Earthquake ruptures with thermal weakening and the operation of major faults at low overall stress levels, *J. Geophys. Res.*, *114*, B07302, doi:10.1029/2008JB006143, 2009.
Noda, H., and N. Lapusta, Three-dimensional earthquake sequence simulations with evolving temperature and pore pressure due to shear heating: Effect of heterogeneous hydraulic diffusivity, *J. Geophys. Res.*, *115*(B12), doi:10.1029/2010JB007780, 2010.
Noda, H., and N. Lapusta, Stable creeping fault segments can become destructive as a result of dynamic weakening, *Nature*, 1–6, doi:10.1038/nature11703, 2013.
Perrin, G., J. R. Rice, and G. Zheng, Self-healing slip pulse on a frictional surface, *J. Mech. Phys. Solids*, **43**, 1461-1495, 1995.
Perry, S. and N. Lapusta. Reproducing magnitude-invariant stress drops in fault models with thermal pressurization (oral presentation), *The 24th International Congress of Theoretical and Applied Mechanics*, Montréal, Québec, Canada, Aug. 2016. (Extended abstract and oral presentation)
Rice, J. R. and A. L. Ruina, Stability of steady frictional slipping, *J. Appl. Mech.*, **50**, 343-349, 1983.
Rice, J. R., Heating and weakening of faults during earthquake slip, *J. Geophys. Res*., doi:10.1029/2005JB004006, 2006.
Rice, J. R., N. Lapusta, and K. Ranjith, Rate and state dependent friction and the stability of sliding between elastically deformable solids, *J. Mech. Phys. Solids* 49, 1865-1898, 2001.
Rolandone, F., R. Bürgmann, and R. M. Nadeau (2004), The evolution of the seismic- aseismic transition during the earthquake cycle: Constraints from the time-dependent depth distribution of aftershocks, *Geophys*. *Res*. *Lett*., *31(23)*, L23,610, doi: 10.1029/2004GL021379.
Rubin, A.M., and J.-P. Ampuero, Earthquake nucleation on (aging) rate and state faults, *J. Geophys. Res.,* 110, doi:10.1029/2005JB003686, 2005.
Rubinstein, J.L., W.L. Ellsworth, K.H. Chen, and N. Uchida, The time and slip-predictable models cannot be dependably used to predict earthquake behavior 1: Repeating earthquakes, *J. Geophys. Res.,*117, B02306, doi:10.1029/2011JB008724, 2012.
Ruina, A. L., Slip instability and state variable friction laws, *J. Geophys. Res*., **88**, 10359-10370, 1983.
Sammis, C. G., Nadeau, R. M., & Johnson, L. R. How strong is an asperity?. *J. Geophys Res*, **104** (B5), 10609-10619, 1999.

Sammis, C. G., and J. R. Rice, Repeating earthquakes as low-stress-drop events at a border between locked and creeping fault patches, *Bull. Seism. Soc. Am.,* 91, 3, 532-537, 2001.

Sato, T., and T. Hirasawa, Body wave spectra from propagating shear cracks, *J. Phys. Earth*, **21**, 415–431, 1973.

Schaff, D. P., G. C. Beroza, and B. E. Shaw, Postseismic response of repeating aftershocks, *Geophys. Res. Lett*., **25**, 4549– 4552, 1998.

Schaff, D. P., and G. C. Beroza, Coseismic and postseismic velocity changes measured by repeating earthquakes, *J. Geophys. Res*., **109**, B10302, doi:10.1029/2004JB003011, 2004.

Schaff, D. P., G. Bokelmann, G. C. Beroza, F. Waldhauser, and W. L. Ellsworth (2002), High-resolution image of Calaveras Fault seismicity, *J. Geophys. Res. Solid Earth*, *107*(B9), –ESE 5–16, doi:10.1029/2001JB000633.

Scholz, C. H. Earthquakes and friction laws. *Nature* **391**, 37–42, 1998.

Schulz, S. S., Catalog of Creepmeter Measurements in California from 1966 through 1988, USGS Open-File Report. USGS, 1989.

Sibson, R. H., Interaction between temperature and pore-fluid pressure during earthquake faulting and a mechanism for partial or total stress relief, *Nature*, **243**, 66–68, 1973.

Shaw, B. E., and S. G. Wesnousky, Slip-Length Scaling in Large Earthquakes: The Role of Deep-Penetrating Slip below the Seismogenic Layer, *Bull. Seismol. Soc. Amer.*, *98*(4), 1633–1641, doi:10.1785/0120070191, 2008.

Tsutsumi, A. & Shimamoto, T. High velocity frictional properties of gabbro. *Geophys. Res. Lett.* **24**, 699–702, 1997.

Tullis, T. E., Friction of Rock at Earthquake Slip Rates, in *Treatise on Geophysics*, vol. 4, Earthquake Seismology, edited by H. Kanamori, Elsevier, Amsterdam, 2007.

Vidale, J. E., Ellsworth, W. L., Cole, A., and C. Marone, Variations in rupture process with recurrence interval in a repeated small earthquake, *Nature*, 368, 6472, 624-626, 1994.